Whole-brain macromolecular tissue volume mapping: A comparison of imaging readouts at 3 Tesla

Francesco Grussu[1,2]*, Marco Battiston[2], Ferran Prados[2,3], Torben Schneider[4], Enrico Kaden[1], Sébastien Ourselin[3], Rebecca S. Samson[2], Daniel C. Alexander[1], Claudia A. M. Gandini Wheeler-Kingshott[2,5,6]

[1]Centre for Medical Image Computing, Department of Computer Science, University College London, London, United Kingdom
[2]Queen Square MS Centre, UCL Queen Square Institute of Neurology, Faculty of Brain Sciences, University College London, London, United Kingdom
[3]Centre for Medical Image Computing, Department of Medical Physics and Biomedical Engineering, University College London, London, United Kingdom
[4]Philips UK, Guildford, Surrey, United Kingdom
[5]Brain MRI 3T Research Center, IRCCS Mondino Foundation, Pavia, Italy
[6]Department of Brain and Behavioral Sciences, University of Pavia, Pavia, Italy
*f.grussu@ucl.ac.uk

INTRODUCTION

Measuring macromolecular content in the human brain non-invasively can provide important diagnostic and prognostic indicators in a number of neurological conditions [1]. In white matter, for instance, alterations of the macromolecular content are indicative of changes in myelin content, observed in certain diseases including but not limited to multiple sclerosis [2]. Also, measuring the myelination of axons in vivo can provide important information about neuronal function, with important implications in neuroscience and in the study of neuroanatomy and neurophysiology.

Quantitative magnetic resonance imaging (MRI) enables the in vivo measurement of properties related to tissue microstructure, such as the macromolecular tissue volume (MTV). To date, MTV-mapping has been based mainly on gradient echo (GE) imaging [1-6], as this provides high resolution and high signal-to-noise ratio. However, routine GE readouts differ considerably from those employed for diffusion MRI (i.e. echo planar imaging or EPI), as they exhibit different distortions and susceptibility to physiological noise and artifacts. In practice, this can limit

the correspondence of spatial features in multi-modal imaging, such as g-ratio mapping [4, 6, 7], where myelin sensitive markers (such as MTV) are combined with diffusion-derived estimates of axonal density on a voxel-by-voxel basis.

In this work, we compare two approaches for clinically feasible MTV mapping of the whole brain: one based on conventional GE imaging [2, 3, 5], and one based on EPI. Specifically, deriving MTV from EPI readouts could be potentially useful in multi-modal approaches where diffusion MRI is to be used (diffusion MRI relies heavily on EPI), and is compatible with state-of-the-art multi-band accelerations [8]. Here, we explore the potential of EPI-based MTV mapping, deriving MTV from quantitative proton density (PD) and relaxation time constants.

METHODS

Imaging

2 healthy volunteers (2 males, age 28 and 29) were scanned on a 3 Tesla Philips Achieva MRI system using both a 3D spoiled GE vs multi-slice spin echo EPI MTV-mapping protocol, with the two protocols matched for scan time. GE imaging relied on a variable flip angle (VFA) acquisition (including actual flip angle measurements [9]) and T2* measurements, while the EPI protocol relied on state-of-the-art inversion recovery (IR) imaging [10] and T2 measurements. Each protocol was acquired twice, in two separate sessions (4 sessions in total: 2 GE; 2 EPI), which also included the same standard T1-weighted anatomical image (resolution of 1x1x1 mm3). Figure 1 reports the salient parameters of the GE and EPI protocols.

MTV calculation

MTV was calculated as MTV = 1 − qPD, where qPD is the quantitative PD, normalised to that of brain ventricles (i.e. water). qPD was obtained from the apparent PD via removal of receiver chain spatial bias based on quantitative T1 values, while accounting for macroscopic T2 (for EPI) and macroscopic T2* (GE) weighting [3]. Quantitative T1 values were derived from the VFA data for GE imaging (correcting nominal flip angles voxel-by-voxel), while T1 was measured with IR for EPI [11].

Protocol	TE [ms]	TR [ms]	Resolution FH×AP×RL [mm3]	FOV FH×AP×RL [mm3]	Readout	Parameters for quantitative imaging	Total scan time [min:s]
GE	2.4	18	1.0×1.0×1.0	256×240×170	3D readout; half-scan factor 0.625; BW = 246 KHz; SENSE = 2	2 flip angles (4° and 25°) for T1 mapping; 6 echoes (2.4, 4.8, 7.2, 9.6, 12.0, 14.4) for T2* mapping	12:57
EPI	34	12000	2.5×2.5×2.5	125×222×192	2D readout; single-shot; EPI factor 47; BW = 642 KHz; SENSE = 2	10 linearly spaced TI in [40; 4000] ms for T1 mapping; 4 echoes (45, 70, 95, 200 ms) for T2 mapping	11:40

FIGURE 1: Salient parameters of the GE (gradient echo) and spin echo EPI (echo planar imaging) protocols implemented in this work. The scan time of the GE protocol includes B1 mapping performed with the actual flip angle method [9].

Analysis

For each subject and scan, the VFA and EPI scans were linearly co-registered to the anatomical T1-weighted image. Subsequently, we generated a mid-way space between scan and rescan using the anatomical images and affine co-registration. Finally, quantitative metrics (MTV and quantitative T1 maps) were warped to the mid-way space, whereby each map was then resampled to the EPI resolution. All co-registrations were performed using NiftyReg [12].

Scan-rescan mean MTV and T1 provided by the GE and EPI protocols were compared voxel-by-voxel by evaluating distributions of values in white and grey matter.
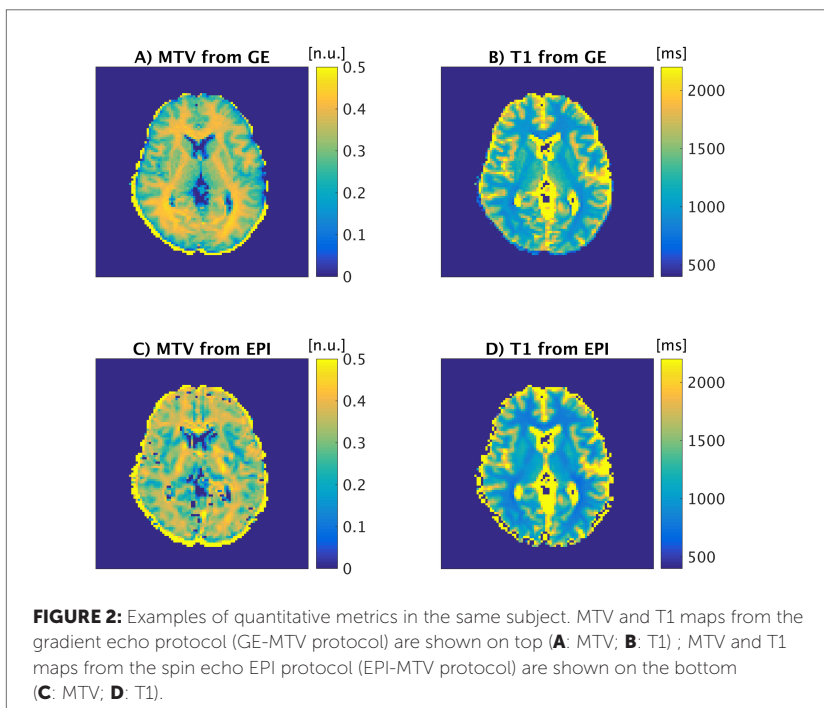
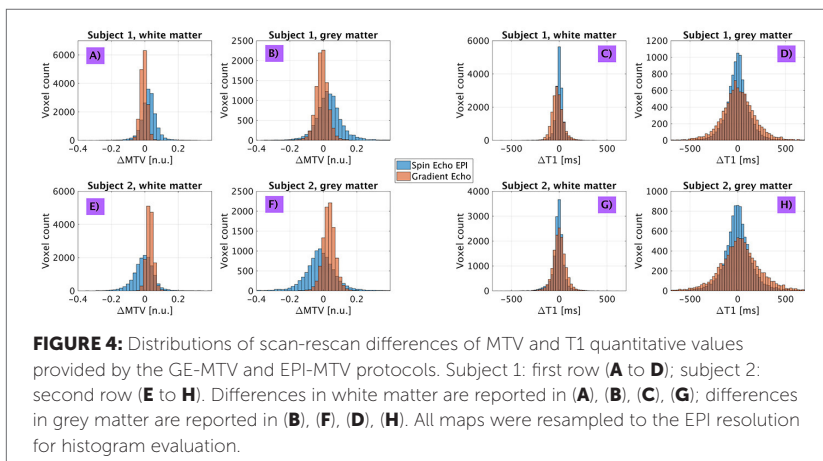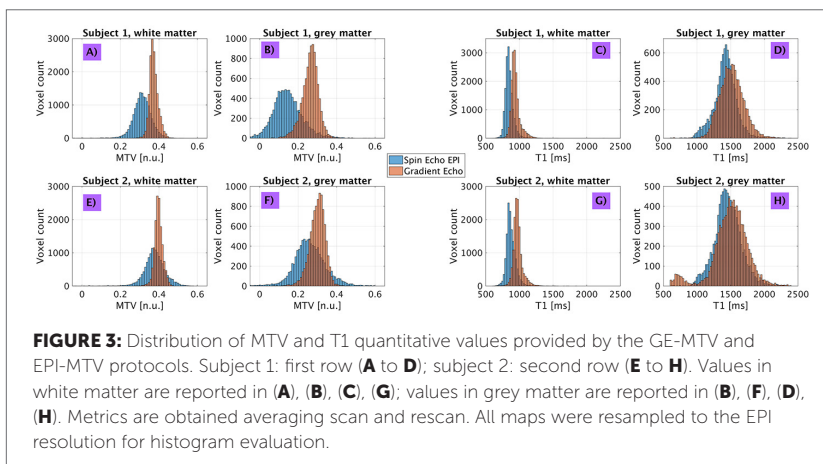Scan-rescan differences between MTV and T1 were also calculated, and characterised via histograms.

For our analysis, we segmented white and grey matter on the reference anatomical images and warped the segmentations to the mid-way space. Segmentations were obtained using the geodesic information flow algorithm [13].

RESULTS AND DISCUSSION

Figure 2 shows examples of quantitative maps of MTV and T1 obtained from the 2 protocols (GE and EPI), while figure 3 shows distributions of MTV and T1 values obtained from the two protocols.

Both the GE and EPI protocols provide MTV that is lower in GM than in WM, as expected given its known lower macromolecular (myelin) content [3]. EPI provides slightly lower MTV that than GE. MTV maps acquired with EPI also show higher GM/WM contrast and higher within-tissue variability. The voxel-wise maps shown in figure 2 also highlight some other differences between protocols, for instance: MTV in the corticospinal tract is slightly higher in EPI than GE, and EPI is more prone to residual ringing artifacts. Quantitative T1 values obtained from GE (i.e. via VFA imaging) and EPI (i.e. via IR imaging) are

FIGURE 2: Examples of quantitative metrics in the same subject. MTV and T1 maps from the gradient echo protocol (GE-MTV protocol) are shown on top (**A**: MTV; **B**: T1) ; MTV and T1 maps from the spin echo EPI protocol (EPI-MTV protocol) are shown on the bottom (**C**: MTV; **D**: T1).

FIGURE 3: Distribution of MTV and T1 quantitative values provided by the GE-MTV and EPI-MTV protocols. Subject 1: first row (**A** to **D**); subject 2: second row (**E** to **H**). Values in white matter are reported in (**A**), (**B**), (**C**), (**G**); values in grey matter are reported in (**B**), (**F**), (**D**), (**H**). Metrics are obtained averaging scan and rescan. All maps were resampled to the EPI resolution for histogram evaluation.

FIGURE 4: Distributions of scan-rescan differences of MTV and T1 quantitative values provided by the GE-MTV and EPI-MTV protocols. Subject 1: first row (**A** to **D**); subject 2: second row (**E** to **H**). Differences in white matter are reported in (**A**), (**B**), (**C**), (**G**); differences in grey matter are reported in (**B**), (**F**), (**D**), (**H**). All maps were resampled to the EPI resolution for histogram evaluation.

qualitatively similar, although T1 from GE (i.e. VFA) is 10%-20% higher than from EPI (i.e. IR), in agreement with previous reports [11].

Figure 4 shows scan-rescan differences for MTV and T1 provided by the GE and EPI protocols. There is a good scan-rescan agreement for quantitative T1 for both GE and EPI protocols, although T1 from EPI is slightly more stable

(narrower distributions). MTV measurement is less repeatable, and systematic scan-rescan differences are seen for both GE and EPI protocols. While this may be partly due to different levels of hydration between scan and rescan (performed on separate days), systematic instrumental/algorithm effects may also have contributed.

CONCLUSIONS

MTV mapping based on an EPI readout is a feasible alternative to conventional measurement based on GE imaging. While EPI MTV shows slightly higher variability than its GE-derived counterpart, the EPI readout enables more stable quantitative T1 measurements via state-of-the-art slice shuffling, which are also promising for the characterisation of diffuse pathology [2]. In the future, we plan to integrate simultaneous multi-slice imaging to our EPI protocol to further improve its performance.

ACKNOWLEDGEMENT

REFERENCES

1. Mezer, A., et al., Quantifying the local tissue volume and composition in individual brains with magnetic resonance imaging. Nature Medicine, 2013. 19(12): p. 1667-1672.
2. Gracien, R.M., et al., Multimodal quantitative MRI assessment of cortical damage in relapsing-remitting multiple sclerosis. Journal of Magnetic Resonance Imaging, 2016. 44(6): p. 1600-1607.

3. Volz, S., et al., Quantitative proton density mapping: correcting the receiver sensitivity bias via pseudo proton densities. NeuroImage, 2012. 63(1): p. 540-552.

4. Duval, T., et al., g-Ratio weighted imaging of the human spinal cord in vivo. NeuroImage, 2017. 145: p. 11-23.

5. Mezer, A., et al., Evaluating quantitative proton-density-mapping methods. Human Brain Mapping, 2016. 37(10): p. 3623 3635.

6. Berman, S., et al., Evaluating g-ratio weighted changes in the corpus callosum as a function of age and sex. NeuroImage 2018. 182: p. 304-313.

7. Stikov, N., et al., In vivo histology of the myelin g-ratio with magnetic resonance imaging. NeuroImage, 2015. 118: p. 397 405.

8. Feinberg, D.A. and K. Setsompop, Ultra-fast MRI of the human brain with simultaneous multi-slice imaging. Journal of Magnetic Resonance, 2013. 229: p. 90-100.

9. Yarnykh, V.L., Actual flip-angle imaging in the pulsed steady state: a method for rapid three-dimensional mapping of the transmitted radiofrequency field. Magnetic Resonance in Medicine, 2007. 57(1): p. 192-200.

10. Battiston, M., et al., Fast and reproducible in vivo T1 mapping of the human cervical spinal cord. Magnetic Resonance in Medicine 2018. 79(4): p. 2142-214.

11. Stikov, N., et al., On the accuracy of T1 mapping: searching for common ground. Magnetic Resonance in Medicine, 2015. 73(2): p. 514-522.

12. Ourselin, S., et al., Reconstructing a 3D structure from serial histological sections. Image and Vision Computing, 2001. 19(1): p. 25-31.

13. Cardoso, M.J., et al., Geodesic information flows: spatially-variant graphs and their application to segmentation and fusion. IEEE Transactions on Medical Imaging, 2015. 34(9): p. 1976-1988.